Lithos 248–251 (2016) 353–365

Contents lists available at ScienceDirect

Lithos

journal homepage: www.elsevier.com/locate/lithos

I-type granitoids associated with the early Paleozoic intracontinental orogenic collapse along pre-existing block boundary in South China

Yang Yu [a,b], Xiao-Long Huang [a,*], Peng-Li He [a,c], Jie Li [a,c]

[a] State Key Laboratory of Isotope Geochemistry, Guangzhou Institute of Geochemistry, Chinese Academy of Sciences, Guangzhou 510640, China
[b] Department of Earth Sciences, The University of Hong Kong, Pokfulam Road, Hong Kong, China
[c] University of Chinese Academy of Sciences, Beijing 100049, China

ARTICLE INFO

Article history:
Received 19 August 2015
Accepted 2 February 2016
Available online 12 February 2016

Keywords:
Mafic microgranular enclaves
I-type granite
Pre-existing block boundary
Intracontinental orogen
Eastern Yangtze Block
Cathaysia Block

ABSTRACT

The early Paleozoic Wuyi–Yunkai orogeny resulted in extensive magmatism in the Cathaysia and eastern Yangtze blocks, South China. Identifying the nature of related magmatism is essential for understanding the orogeny that remains enigmatic with regard to its tectonic setting and geodynamic driving force. The Zhangjiafang pluton (438 ± 3 Ma) in western Jiangxi province is composed of predominant granodiorite with abundant coeval mafic-intermediate microgranular enclaves (MMEs) (~433 ± 5 Ma). The granodiorite samples are weakly peraluminous (A/CNK = 1.05–1.09) and have low SiO_2 (61.9–64.9 wt.%) and high Fe_2O_3 (4.6–5.6 wt.%), MgO (2.2–2.8 wt.%) and CaO (4.3–4.8 wt.%), belonging to I-type suite due to abundant amphibole in the rocks. They exhibit strongly negative whole-rock $\varepsilon_{Nd}(t)$ values (−11 to −9) and zircon $\varepsilon_{Hf}(t)$ values (−14 to −4), similar to the basement of the Cathaysia Block, but distinguishable from simultaneous I-type granites of the Banshanpu and Hongxiaqiao plutons in eastern Yangtze Block in much lower Sr, Ba, Th and U. The MME samples show pronounced negative Nb–Ta–Ti anomalies and have overall less negative whole-rock $\varepsilon_{Nd}(t)$ (−9 to −7) and zircon $\varepsilon_{Hf}(t)$ values (−9 to −4) than the host granodiorite, which are best interpreted as products of mantle-derived melts that mixed insufficiently with crust-derived magma.

The block boundary between the eastern Yangtze and Cathaysia blocks should pass through the nearby west area (i.e., Pingxiang City) of the Zhangjiafang pluton. The Early Paleozoic I-type granitic rocks near the block boundary have all negative $\varepsilon_{Nd}(t)$ and $\varepsilon_{Hf}(t)$ values, demonstrating an overall ancient basement of the two blocks prior to the Wuyi–Yunkai orogeny, preferring an intracontinental orogeny model. However, the early Paleozoic mafic rocks and I-type granites with coeval MMEs were frequently present along the Jiangshan–Shaoxing–Pingxiang Fault zone, illustrating widespread modification of the ancient basement adjacent to the block boundary by mantle-derived melt during the orogenic collapse. The pre-existing block boundary might have promoted asthenosphere upwelling and basaltic underplating during the intracontinental orogenic collapse.

1. Introduction

The South China Block (SCB) consists of the Yangtze Block in the northwest and the Cathaysia Block in the southeast, which have distinct basements (e.g., Zhang et al., 2012; Zhao and Cawood, 2012) and were amalgamated during the Early Neoproterozoic (e.g., Li et al., 2006, 2008, 2009; Wang et al., 2007). After that, it underwent at least three major tectonothermal events of the Wuyi–Yuankai orogeny (early-middle Paleozoic), Indosinian event (Triassic) and Yanshanian event (Jurassic–Cretaceous) (e.g., Charvet, 2013; Charvet et al., 2010; Faure et al., 2009; Li et al., 2010; Shu et al., 2014; Wang et al., 2013a). The early Paleozoic Wuyi–Yunkai orogeny, as the first extensive tectonothermal event in South China since the Neoproterozoic break-up of the Rodinia supercontinent (e.g., Chen et al., 1991; Li et al., 2010; Shu et al., 2014; Wang et al., 2011), resulted in the remobilization of basement of the eastern Yangtze and Cathaysia blocks. The reactivation would be due to orogenic collapse, which is progressively revealed by recent investigation on early Paleozoic mafic rocks (Fig. 1b) (Wang et al., 2013b; Yao et al., 2012; Zhang et al., 2015) and I-type granites in the eastern SCB (Fig. 1b) (Guan et al., 2014; Huang et al., 2013; Xia et al., 2014; Zhang et al., 2015). Alternatively, the Wuyi–Yunkai orogeny has been regarded as a consequence of continental or arc collisions with closure of a proposed Huanan Ocean between the eastern Yangtze and Cathaysia blocks (Guo et al., 1989; Hsü, 1994; Hsü et al., 1990; Shui, 1987). However, the most recent work interpreted it as an intraplate orogenic event (e.g., Charvet et al., 2010; Faure et al., 2009; Li et al., 2010; Wang et al., 2007, 2011, 2013a,). Nevertheless, the orogeny remains enigmatic with regard to its tectonic setting and geodynamic driving force (Li et al., 2010; Wang et al., 2013a, 2013b). Identifying

* Corresponding author. Tel.: +86 20 85290010.
E-mail address: xlhuang@gig.ac.cn (X.-L. Huang).

http://dx.doi.org/10.1016/j.lithos.2016.02.002
0024-4937/

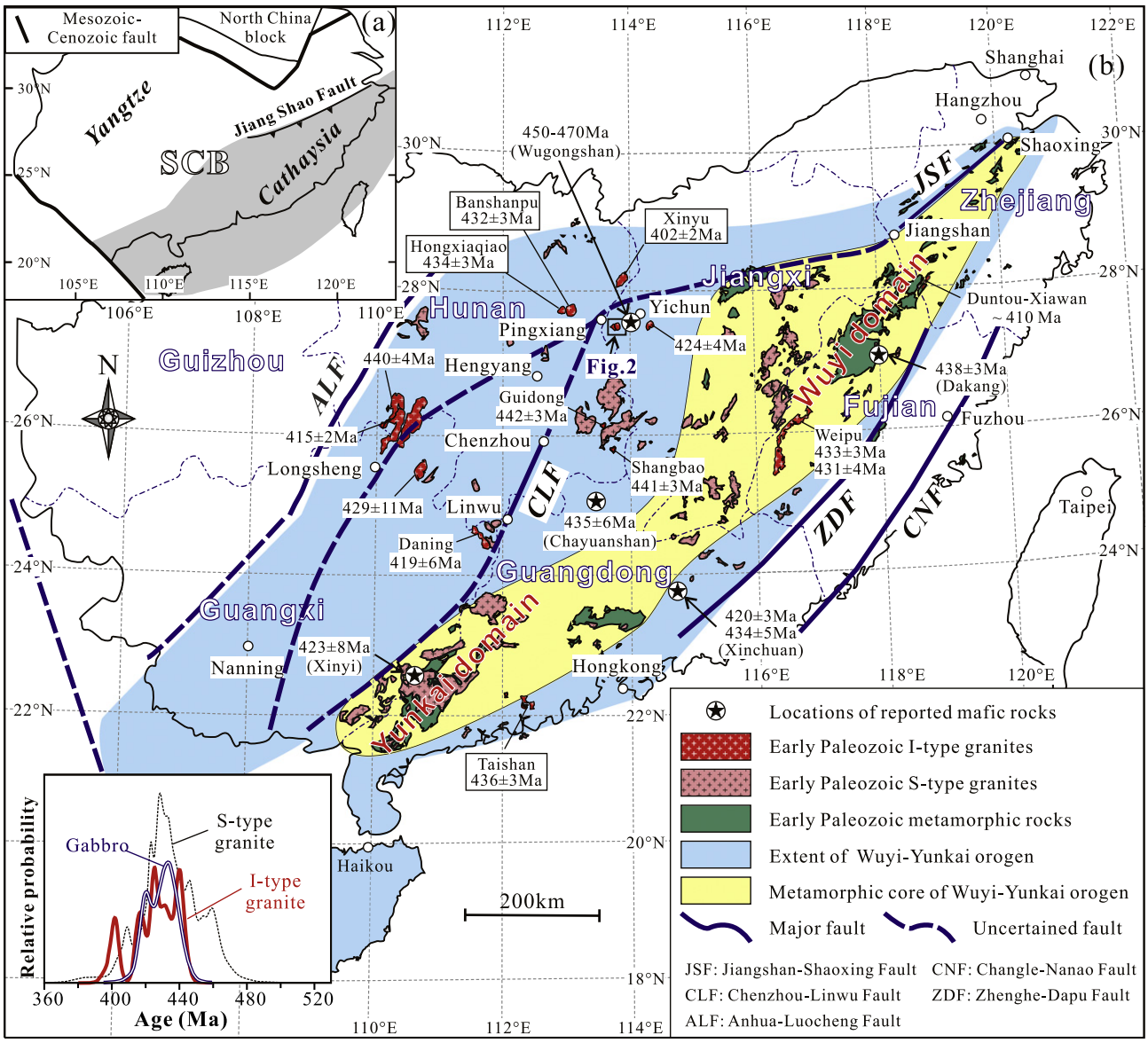

Fig. 1. (a) Simplified regional map highlighting the tectonic framework of the South China Block (SCB) that is made of the Yangtze and Cathaysia blocks (revised from Li et al., 2010). (b) Sketch map showing the known extent of the early Paleozoic Wuyi–Yunkai orogen, the metamorphic core of the orogen, the early Paleozoic granitic rocks of the eastern SCB and the location of known mafic rocks (revised from Li et al., 2010; Wang et al., 2011; Huang et al., 2013). Insert geochronology histogram show the age range of the early Paleozoic mafic and granitic rocks in the eastern SCB. Geochronology data are according to the literatures (Chen et al., 2008; Gan et al., 1993; Guan et al., 2014; Huang et al., 2013; Li et al., 2010; Lou et al., 2005; Peng et al., 2006; Shen et al., 2008; Wan et al., 2007; 2010; Wang et al., 2007, 2011; 2013b; Wu and Zhang, 2003; Xia et al., 2014; Xie and Yang, 2000; Xu and Xu, 2015; Xu et al., 2009; Zhang et al., 2012, 2015; Zhong et al., 2014).

the nature of related magmatism and tectonic boundary between the eastern Yangtze and Cathaysia blocks is essential for understanding the processes responsible for the orogeny.

The early Paleozoic northeastern boundary between the Yangtze and Cathaysia blocks is commonly accepted as the northeasterly striking Jiangshan–Shaoxing Fault (Fig. 1b) for evidence including Neoproterozoic ophiolites (Chen et al., 1991; Yao et al., 2014), arc-type granites (Li et al., 2008) and HP/LT blueschists (Li et al., 2009). However, the middle part of the boundary is still ambiguous and has been largely debated (Fig. 1b) due to poor exposure and strong modification by young tectonic events (Li et al., 2010; Wang et al., 2013a). Recent studies about sedimentology, biofacies and lithofacies suggest that the tectonic boundary would extend from the Shaoxing–Jiangshan–Pingxiang fault zone to the Hengyang and Longsheng areas (Fig. 1b) (Chen et al., 2012; Shu et al., 2015). Whereas, Wang et al. (2003) proposed that the Chenzhou–Linwu Fault could represent the southwestern part of the boundary between the two blocks (Fig. 1b) because the mafic rocks across the fault show distinct geochemical characteristics and define different lithosphere mantle sources across the fault. This is also consistent with recent geophysical data that exhibit different geophysical properties in the crust across the Chenzhou–Linwu Fault (Rao et al., 2012). The early Paleozoic I-type granites in the eastern Yangtze and Cathaysia blocks could record geochemical characteristics of the basements of the two blocks because most of them have resisted the impacts of the later tectonic-thermal events. A cluster of early Paleozoic I-type granites, including the Banshanpu and Hongxiaiqiao plutons to the west, Xinyu pluton to the north and Zhangjiafang pluton to the east of Pingxiang City, are likely outcrops along the middle part of the boundary between the Yangtze and Cathaysia blocks (Fig. 1b), which would be a good opportunity for investigation of the block boundary. Guan et al. (2014) had proposed that the Banshanpu and Hongxiaqiao plutons were derived from partial melting of lower crust with residual garnet in the eastern Yangtze Block. The Zhangjiafang pluton was suspected to be an early Paleozoic I-type granite in the Cathaysia Block (Fig. 1b) (Zhang

et al., 2012). If so, the middle part of the block boundary between the eastern Yangtze and Cathaysia blocks would pass through the narrow area between the Zhangjiafang pluton and the Banshanpu and Hongxiaqiao plutons. However, there is still no geochemical data available for the Zhangjiafang pluton. In this study, we report both the geochronological and geochemical characteristics of the granites and coexisting mafic microgranular enclaves (MMEs) of the Zhangjiafang pluton in order to elucidate the magma sources and petrogenetic processes of the rocks. The results allow us to explore geochemical difference of the basements and outline the block boundary between the eastern Yangtze and Cathaysia blocks, which would also offer new perspectives on the early Paleozoic magmatism associated with the Wuyi–Yunkai orogenic collapse in the SCB.

2. Geological background and sample descriptions

The SCB is bounded by the Qinling–Dabie–Sulu orogenic belt to the north, the Longmenshan Fault to the northwest, the Red River Fault to the southwest, and the continental slope of the East China Sea and the South China Sea to the southeast (Fig. 1a). The basement of the Yangtze Block in the northwest of the SCB consists predominantly of Proterozoic and a small amount of Archean rocks known as the Kongling Complex (e.g., Gao et al., 2011; Qiu et al., 2000). The Archean–Paleoproterozoic crystalline basement was surrounded by Late Mesoproterozoic to Early Neoproterozoic strata, which are locally unconformably overlain by weakly metamorphosed Neoproterozoic strata (i.e., the Banxi Group) and unmetamorphosed upper-Neoproterozoic to Paleozoic succession (Zhao and Cawood, 2012; and references therein). In the eastern Yangtze Block, the oldest outcropped rocks are represented by early Neoproterozoic metamorphosed volcanic-sedimentary units, such as Sibao Group in north Guangxi, Fanjingshan Group in northeast Guizhou, Lengjiaxi Group in central Hunan, Shuangqiaoshan/Jiuling Group in northwest Jiangxi and Shangxi Group in south Anhui (Zhao and Cawood, 2012; and references therein). The Precambrian basement of the Cathaysia Block can be divided into the Wuyishan terrane to the northeast and the Nanling–Yunkai terrane to the southwest (Fig. 1b) (Xu et al., 2005; Yu et al., 2010). Paleoproterozoic granites, metasedimentary and volcanic rocks outcropped in northeastern Wuyishan were supposed to be the basement of the Wuyishan terrane (Liu et al., 2014; Yu et al., 2010). The Silurian strata were missing, and a widespread angular unconformity between the overlying upper Paleozoic terrestrial deposits (Devonian and younger) and the lower Paleozoic meta-sedimentary successions (typically Ordovician and older) could be recognized in the southeast part of the SCB (Shu et al., 2014).

The Zhangjiafang pluton to the east of Pingxiang City (Fig. 1b) intruded into the Neoproterozoic metasedimentary sequence or early Paleozoic gneissic granites (Fig. 2) with ages mainly of 440–456 Ma (Wang et al., 2011). The Zhangjiafang pluton is predominantly composed of granite in the eastern part and granodiorite in the western part (Fig. 2) that show gradual transition without sharp boundary. There are abundant mafic microgranular enclaves (MMEs) hosted in the granodiorite (Fig. 3a, b). The granodiorite samples are porphyritic, and plagioclase phenocrysts are mostly euhedral–subhedral and zoned (Fig. 3c). The common mineral assemblage is biotite (20–30%), amphibole (~15%), plagioclase (25–30%), K-feldspar (10–15%) and quartz (10–15%) (Fig. 3c), with minor accessory minerals of apatite, sphene and magnetite. The fine-grained MMEs are generally elliptic and contact sharply with the host granodiorite (Fig. 3a, b). However, the MMEs often contain variable amounts of large-grained xenocrysts or clots of quartz and feldspars, and some locally show intrusion of host granitoid veinlets (Fig. 3b). The mineral assemblage of MMEs is similar to that of the host granodiorite but has higher proportions of biotite (25–30%), amphibole (~20%) and plagioclase (30–35%) with equal K-feldspar (10–15%) and lower quartz (~10%) (Fig. 3d).

3. Analytical methods

Zircons were separated using conventional heavy liquid and magnetic techniques and purified by the handpicking under a binocular microscope, and cast into an epoxy mount. The mount was then polished to exposure the grain centers and carbon-coated. The internal structures of the zircons were examined using cathodoluminescence (CL) image prior to U–Pb isotopic analysis. Zircon U–Pb analyses were performed using an Agilent 7500a ICP-MS, equipped with a RESOlution M-50 laser-ablation system at the Guangzhou Institute of Geochemistry, Chinese Academy of Sciences (GIG-CAS). Spot sizes of 30 μm with a laser

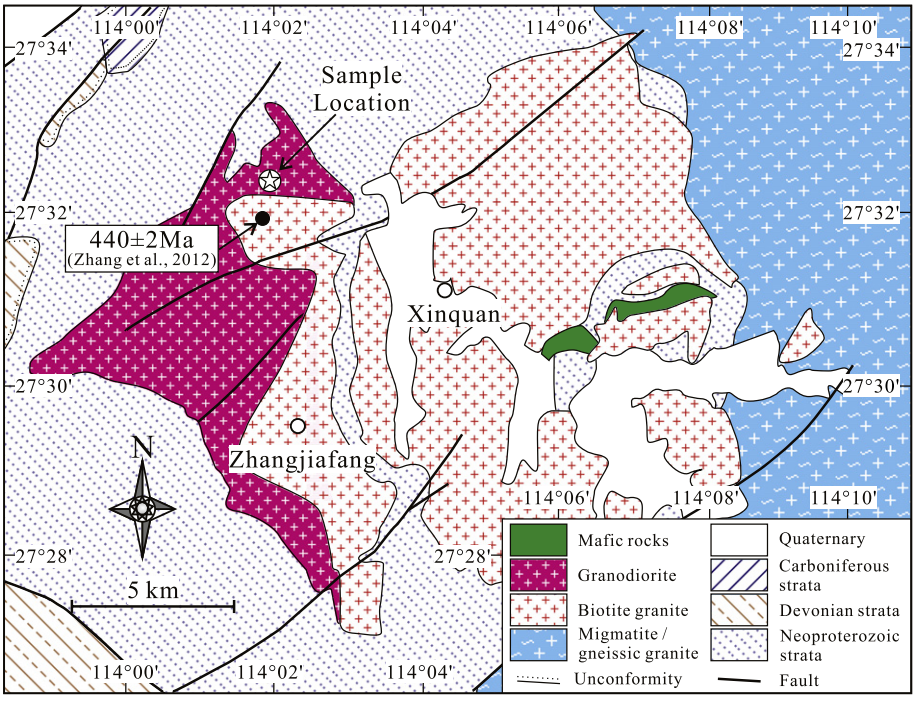

Fig. 2. Simplified geological map of the Zhangjiafang pluton (modified after Yichun and Zhuzhou Geological Maps at 1:200,000 scale), showing rock types and sample location.

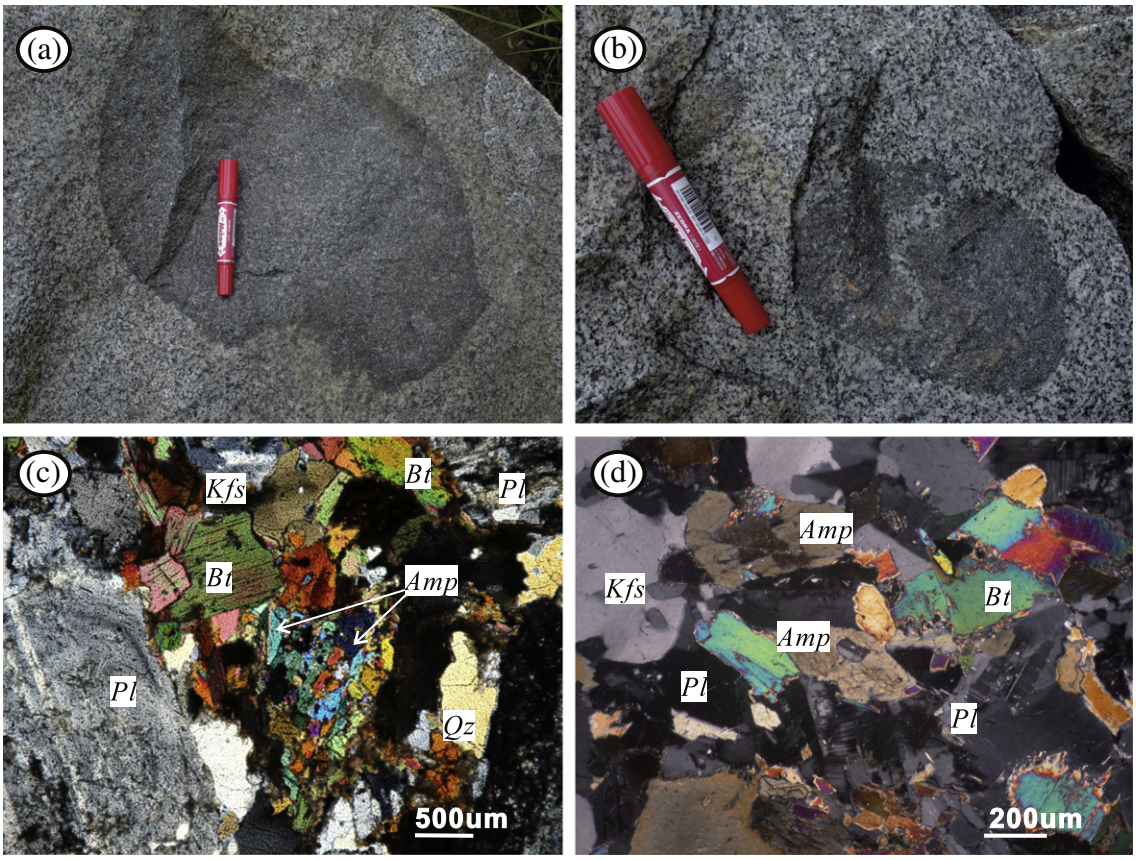

Fig. 3. Field photographs and petrographic characteristics of the Zhangjiafang granodiorite and coexisting mafic microgranular enclave (MME): (a, b) outcrops of elongated MME in the granodiorite; (c) petrographic characteristics of granodiorite (XQ-1); and (d) petrographic characteristics of MME (XQ-15). Mineral abbreviations: Amphibole (Amp), Biotite (Bt), Plagioclase (Pl), K-feldspar (Kfs) and Quartz (Qz). The length of the marker pen in (a) and (b) is ca 14 cm.

frequency of 8 Hz were used. U–Th–Pb ratios and U concentration were determined relative to TEMORA zircons (Black et al., 2003) and the standard NIST610 (Pearce et al., 1997), respectively. Raw count rates were measured for ^{29}Si, ^{204}Pb, ^{206}Pb, ^{207}Pb, ^{208}Pb, ^{232}Th and ^{238}U, $^{207}Pb/^{206}Pb$, $^{206}Pb/^{238}U$, $^{207}Pb/^{235}U$ and $^{208}Pb/^{232}Th$ ratios, and then calculated using the ICP-MS DataCal 6.7 (Liu et al., 2008). The detailed analytical techniques are described in Tu et al. (2011). Uncertainties of individual analyses are reported at the 1σ level, and data reduction was carried out using Isoplot (ver. 3.23) (Ludwig, 2003).

In situ zircon Hf isotopic analyses were carried out on the dated sites using a Neptune MC-ICPMS, equipped with a 193 nm laser, at the Institute of Geology and Geophysics, Chinese Academy of Sciences (IGG-CAS). Spot sizes of 44 μm with a laser repetition rate of 8 Hz were used, which obtained a signal intensity of ~ 5 V at ^{180}Hf mass with the energy density of 15 J/cm^2. The detailed analytical technique and data correction procedures are described in Wu et al. (2006). The mean β_{Yb} ($^{172}Yb/^{173}Yb$) value obtained from zircon itself was applied for the interference correction of ^{176}Yb and ^{176}Lu on ^{176}Hf (Wu et al., 2006). $^{176}Yb/^{172}Yb = 0.5886$ and $^{176}Lu/^{175}Lu = 0.02655$ were used for the elemental fractionation correction. Due to the extremely low $^{176}Lu/^{177}Hf$ in zircon (normally < 0.002 in the studied samples), the isobaric interference of ^{176}Lu on ^{176}Hf is negligible (Iizuka and Hirata, 2005). No relationship between $^{176}Yb/^{177}Hf$ and $^{176}Hf/^{177}Hf$ ratios was observed in the studied samples, indicating that the correction of ^{176}Yb interference on ^{176}Hf is precise for obtaining accurate $^{176}Hf/^{177}Hf$ values. During analysis of the unknown samples, the zircon standard (GJ-1) and Mud Tank gave $^{176}Hf/^{177}Hf$ ratios of 0.282002 ± 25 (2σ; n = 9) and 0.252496 ± 18 (2σ; n = 9), respectively, which are identical with the preferred mean values measured using the LA-MC-ICPMS method (Gerdes and Zeh, 2006; Woodhead et al., 2004). The uncertainties of calibrated isotope ratios, including those from the sample, standards, and reference values, are given at ±2σ. The measured $^{176}Lu/^{177}Hf$ ratios and the ^{176}Lu decay constant of 1.865×10^{-11} yr^{-1} (Scherer et al., 2001) were used to calculate initial $^{176}Hf/^{177}Hf$ ratios. The chondritic values of $^{176}Hf/^{177}Hf = 0.0332$ and $^{176}Lu/^{177}Hf = 0.282772$ (Blichert-Toft and Albarede, 1997) were used for the calculation of ε_{Hf} values.

Whole rock geochemical and Sr–Nd isotopic analyses were carried out at the GIG-CAS. Major element oxides were analyzed using a Rigaku RIX 2000 X-ray fluorescence spectrometer (XRF), and analytical uncertainties are mostly between 1% and 5% (Li et al., 2006). Trace elements were obtained by inductively coupled plasma-mass spectrometry (ICP-MS) after acid digestion of samples in high-pressure Teflon vessels, and detailed procedures are same as those described by Li et al. (2006). The USGS and Chinese National standards AGV-2, GSR-1, GSR-2, MRG-1, BCR-1, W-2 and G-2 were chosen for calibrating element concentrations of the analyzed samples. Analytical precision of REE and other incompatible element analyses is typically 1–5%. Sr and Nd isotopic ratios were measured on a subset of whole-rock samples using a Micro mass Isoprobe multicollector ICP-MS (MC-ICP-MS). Detailed procedures of sample preparation and chemical separation are same as those described by Liang et al. (2003) and Wei et al. (2002). The procedure blanks were in the range of 200–500 pg for Sr and ≤50 pg for Nd. REEs were separated using the cation exchange columns, and the Nd fractions were further separated by HDEHP-coated Kef columns. Measured $^{143}Nd/^{144}Nd$ ratios were normalized to $^{146}Nd/^{144}Nd = 0.7219$. Reference standards were analyzed along with samples and gave $^{87}Sr/^{86}Sr = 0.710273 \pm 18$ (2σ) for NBS987 and $^{143}Nd/^{144}Nd = 0.512094 \pm 11$ (2σ) for Shin Etsu JNdi-1, which are comparable to the recommended values of NBS987 ($^{87}Sr/^{86}Sr = 0.710248$; McArthur, 1994) and Shin Etsu JNdi-1 ($^{143}Nd/^{144}Nd = 0.512115 \pm 7$; Tannaka et al., 2000).

4. Results

4.1. Zircon U–Pb geochronology and Hf isotope

Two granodiorite samples (XQ10-3 and XQ10-13) and one MME sample (XQ10-15) were selected for zircon U–Pb dating (Supplemental Table 1) and Hf isotope analysis (Supplemental Table 2). Zircons are all euhedral prismatic grains, and CL images show strong oscillatory zoning, indicating the magmatic origin.

4.1.1. Granodiorite

The zircons from granodiorite sample XQ10-3 contain variable Th and U contents (39–185 ppm and 132–1050 ppm, respectively) with Th/U ratios of 0.10–0.57 (Supplemental Table 1). Spot 18 on the inherited zircon has an old $^{206}Pb/^{238}U$ age of 760 ± 27 Ma with high U (1050 ppm; Supplemental Table 1). Spots 04, 05 and 21 have slightly old $^{206}Pb/^{238}U$ ages ranging from 465 ± 8 Ma to 482 ± 9 Ma (Fig. 4), which would be mixture between inner inherited zircon and outer magmatic zircon based on the CL images (Fig. 4b). Spots 08 and 11 show slightly young $^{206}Pb/^{238}U$ ages (403 ± 6 Ma and 415 ± 7 Ma, respectively; Supplemental Table 1), possibly due to the later thermal disturbance of U–Pb isotopic system. The other 18 analyses show similar $^{206}Pb/^{238}U$ ages ranging from 427 ± 6 Ma to 451 ± 8 Ma (Supplemental Table 1) with a weighted mean value of 438 ± 3 Ma (MSWD = 0.83; Fig. 4a, b), identical to the age of biotite granite in eastern part of the pluton (440 ± 2 Ma; Fig. 2; Zhang et al., 2012) within errors. All zircons have negative $\varepsilon_{Hf}(t)$ values from −14 to −7 (Fig. 5; Supplemental Table 2).

Twenty-five zircons from granodiorite sample XQ10-13 have variable Th and U contents (50–665 ppm and 165–1805 ppm, respectively) with Th/U of 0.2–0.8 (Supplemental Table 1). Spots 01, 04 and 13 show slightly older apparent $^{206}Pb/^{238}U$ ages (456 ± 7 Ma, 459 ± 7 Ma and 465 ± 9 Ma, respectively; Supplemental Table 1) than the others, which would be derived from the surrounding gneissic granites that have abundant zircons with the crystallization age of > 450 Ma (Wang et al., 2011). The other 22 zircon grains have similar $^{206}Pb/^{238}U$ ages (422 ± 6 to 446 ± 7 Ma; Supplemental Table 1) with a weighted mean value of 438 ± 3 Ma (MSWD = 0.98; Fig. 4c), identical to weighted mean $^{206}Pb/^{238}U$ age of sample XQ10-13 and was interpreted as the crystallization age of the Zhangjiafang granodiorite. These zircons show wide range of negative $\varepsilon_{Hf}(t)$ values (−14 to −4; Fig. 5; Supplemental Table 2).

4.1.2. MME

The zircon grains of MME sample XQ10-15 contain variable Th and U contents (37–229 ppm and 93–1049 ppm, respectively) with relatively low Th/U ratios of 0.1–0.4 (Supplemental Table 1). Spot 09 has older age

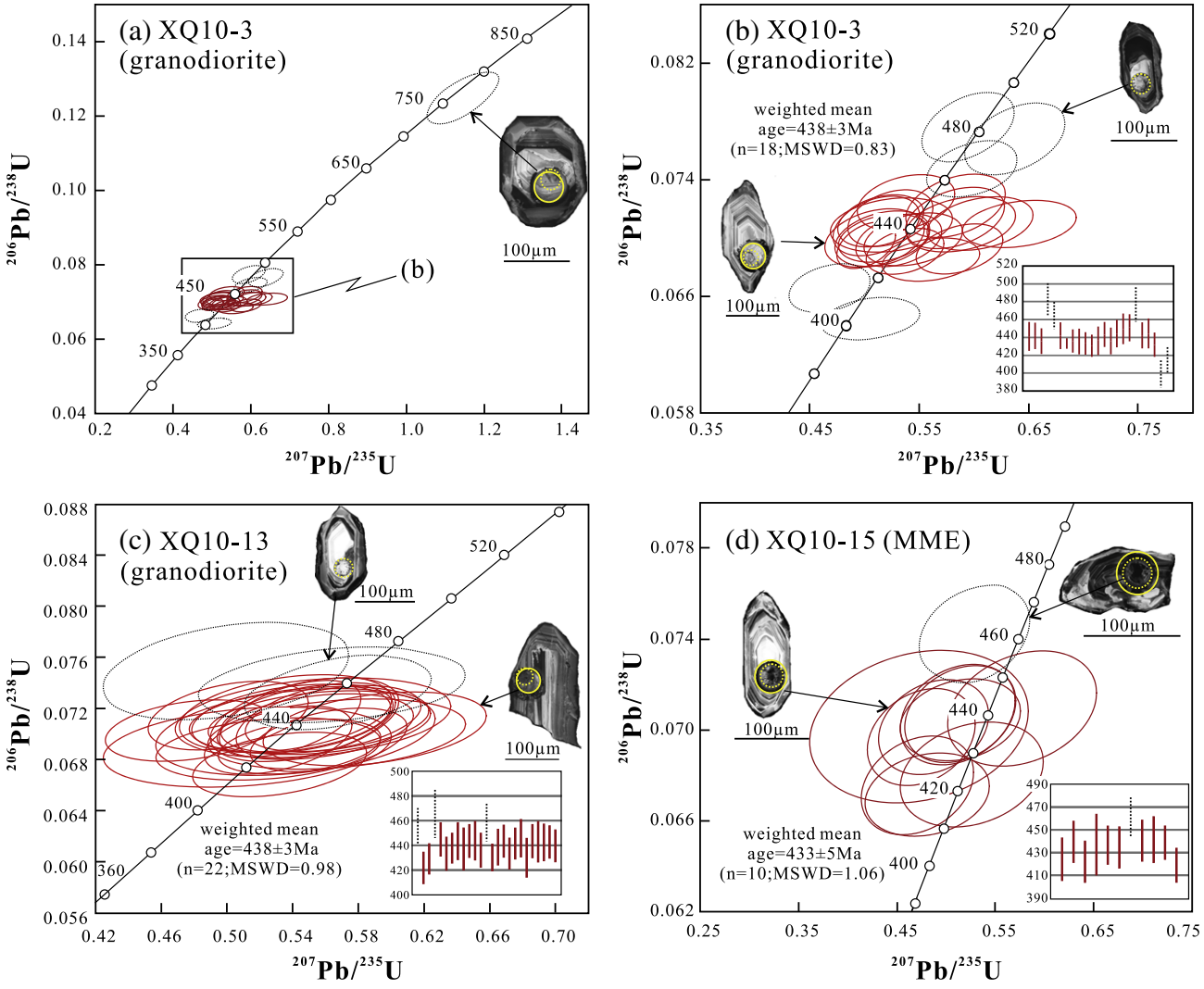

Fig. 4. Concordia diagrams for LA-ICP-MS zircon analyses and diagrams for weighted mean $^{206}Pb/^{238}U$ age of Zhangjiafang granodiorites and MME: (a, b) granodiorite (XQ10-3); (c) granodiorite (XQ10-13); and (d) MME (XQ10-15). The circles on representative CL images denote the locations for in situ zircon U–Pb dating (dotted line) or Lu–Hf isotopic analyses (solid line). Uncertainties of individual analyses are at the 1σ level.

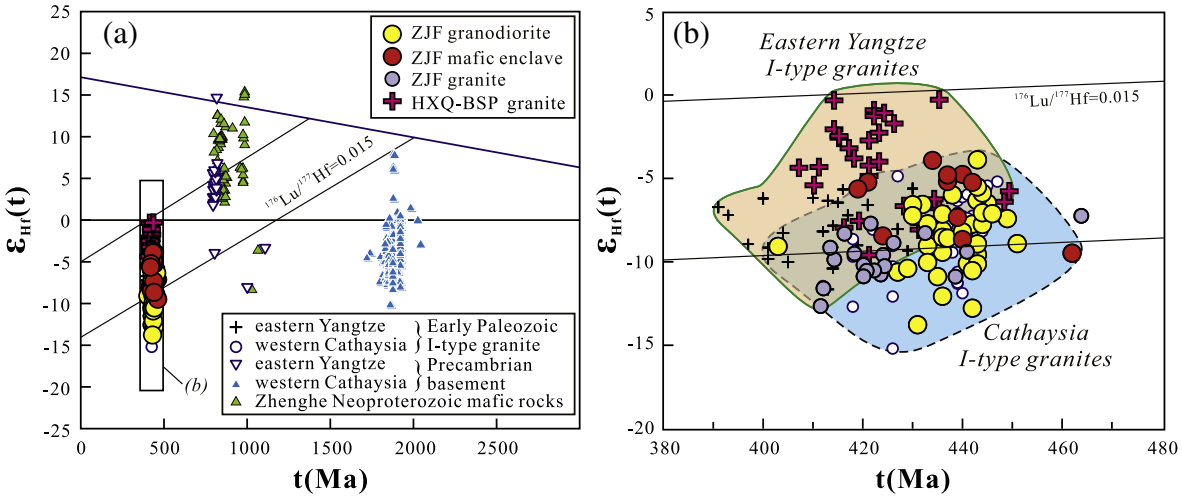

Fig. 5. Diagrams of zircon Hf isotope evolution for Zhangjiafang granodiorites and MMEs. The data sources: the early Paleozoic I-type granites (Zhang et al., 2012) and Precambrian basements (Liu et al., 2014; Shu et al., 2011; Wang et al., 2012, 2013c; Yu et al., 2009; Zhao et al., 2014) of the eastern Yangtze and western Cathaysia blocks, Zhenghe Neoproterozoic mafic rocks (Shu et al., 2011; Wang et al., 2013a, 2013b, 2013c), Hongxiaqiao–Banshanpu (HXQ–BSP) granites (Guan et al., 2014) and Zhangjiafang (ZJF) granite (Zhang et al., 2012).

(462 ± 9 Ma) with much higher Th (229 ppm) and U (1049 ppm) compared to the others, and would be an inherited zircon captured from the surrounding rocks similar to those in granodiorite samples XQ10-3 and XQ10-13. The other ten zircon grains give a weighted mean value of 433 ± 5 Ma (MSWD = 1.06; Fig. 4d), interpreted as the crystallization age of the MMEs, which is equal to the crystallization age of the host granodiorite (438 ± 3 Ma; Fig. 4b, c) within errors. The zircons of the MME sample show overall less negative $\varepsilon_{Hf}(t)$ values (−9 to −4; Fig. 5; Supplemental Table 2) than those of the granodiorite samples.

4.2. Geochemistry

4.2.1. Major and trace elements

Whole-rock major and trace element concentrations of nine granodiorite samples and three MME samples from the Zhangjiafang pluton (Supplemental Table 3) are plotted in Fig. 6, together with surrounding gneissic granites (Wang et al., 2011) and the I-type granite and MMEs from the Banshanpu and Hongxiaqiao plutons in the eastern Yangtze Block (Guan et al., 2014). The Zhangjiafang granodiorites contain low SiO_2 (62–65 wt.%; Supplemental Table 3) and high Al_2O_3 (16.3–17.3 wt.%; Supplemental Table 3), and show a general trend of decreasing TiO_2, Al_2O_3, MgO, CaO, Fe_2O_3 and P_2O_5 with increasing SiO_2 but within narrow ranges (Fig. 6). The MME samples have slightly higher MgO, CaO, Fe_2O_3 and Na_2O but lower P_2O_5, K_2O, SiO_2 and K_2O/Na_2O than the host granodiorites (Fig. 6). The granodiorite samples are weakly peraluminous (A/CNK = 1.00–1.09; Fig. 7), while three MME samples are all metaluminous (A/CNK ≤ 1; Fig. 7), corresponding to higher proportion of amphibole in the MMEs (Fig. 3d).

The Zhangjiafang granodiorites show fractionated chondrite-normalized REE patterns ($[La/Yb]_N$ = 6–29; Supplemental Table 3) with moderately to weakly negative Eu anomalies (Eu/Eu^* = 0.67–1.0; Supplemental Table 3; Fig. 8a). The MME samples have variable REE concentrations and chondrite-normalized REE patterns ($[La/Yb]_N$ = 3–21; $[Dy/Yb]_N$ = 1.8–2.4; Supplemental Table 3) with strongly negative Eu anomalies (Eu/Eu^* = 0.49–0.63; Supplemental Table 3; Fig.8a). On the primitive mantle-normalized multi-element variation diagram, all samples exhibit pronounced negative Nb, Ta, Ti, Sr and Ba anomalies but positive Pb anomaly, similar to the I-type granite and MMEs from the Banshanpu and Hongxiaqiao plutons (Fig. 8b).

4.2.2. Sr–Nd isotopes

The Zhangjiafang granodiorites have low $^{143}Nd/^{144}Nd$ ratios (0.511886–0.511959; Supplemental Table 4) and more negative $\varepsilon_{Nd}(t)$ values (from −11 to −9; Supplemental Table 4) than coeval I-type granites in the eastern Yangtze (Guan et al., 2014; Zhang et al., 2012) and surrounding early Paleozoic gneissic granites (Fig. 9). Initial $^{87}Sr/^{86}Sr$ ratios of the Zhangjiafang granodiorite samples are high in a narrow range of 0.7138–0.7145 (Supplemental Table 4). The MME samples show higher $^{143}Nd/^{144}Nd$ ratios (0.512043–0.512163), less negative $\varepsilon_{Nd}(t)$ values (−9 to −7) and lower initial $^{87}Sr/^{86}Sr$ ratios (0.7127–0.7136) than the host granodiorites (Supplemental Table 4; Fig. 9). All samples likely plot along a mixing curve (Fig. 9) between the Taishan I-type granites (Huang et al., 2013) and Xinyi gabbro (Wang et al., 2013b).

5. Discussion

5.1. Petrogenesis of granodiorite: lower crustal dehydration melting

The Zhangjiafang granodiorite samples show negative $\varepsilon_{Nd}(t)$ values and high $(^{87}Sr/^{86}Sr)_i$ ratios with negative zircon $\varepsilon_{Hf}(t)$ values (Figs. 5, 9), which is clearly distinguished from M-type granite that formed from juvenile mantle-derived materials (Whalen, 1985). The studied samples contain abundant early-crystallizing biotite and amphibole but lack of any peraluminous minerals such as cordierite, muscovite or garnet (Fig. 3c), indicating an overall hydrated and metaluminous feature of their initial magma. Therefore, both petrological and geochemical features denote clearly that the Zhangjiafang granodiorite is not S- or A-type granite but belongs to I-type suite.

Weakly peraluminous or metaluminous feature of the Zhangjiafang granodiorite contradicts with a supracrustal sedimentary source that generally produces strongly peraluminous melts (Lebreton and Thompson, 1988; Vielzeuf and Montel., 1994). Evidently, the studied samples have more negative $\varepsilon_{Nd}(t)$ and higher $(^{87}Sr/^{86}Sr)_i$ (Fig. 9) than the surrounding gneissic granites (i.e., Wugongshan area) that were generated through partial melting of a supracrustal sedimentary source (Wang et al., 2011).

The studied granodiorite samples show narrow ranges of all major elements and uniform trace elements characteristics (Figs. 6, 8), suggesting that they would be products through similar degree of partial melting of the source and have undergone similar fractional crystallization. The rocks might be derived from partial melting of an intermediate to mafic source (e.g., amphibolite; Beard and Lofgren, 1991) according to their high MgO and Fe_2O_3 but low SiO_2 (Fig. 6). Hydrous melting of an intermediate-mafic source usually generates strongly peraluminous melts with extremely high Al_2O_3 (generally >20 wt.% at SiO_2 =

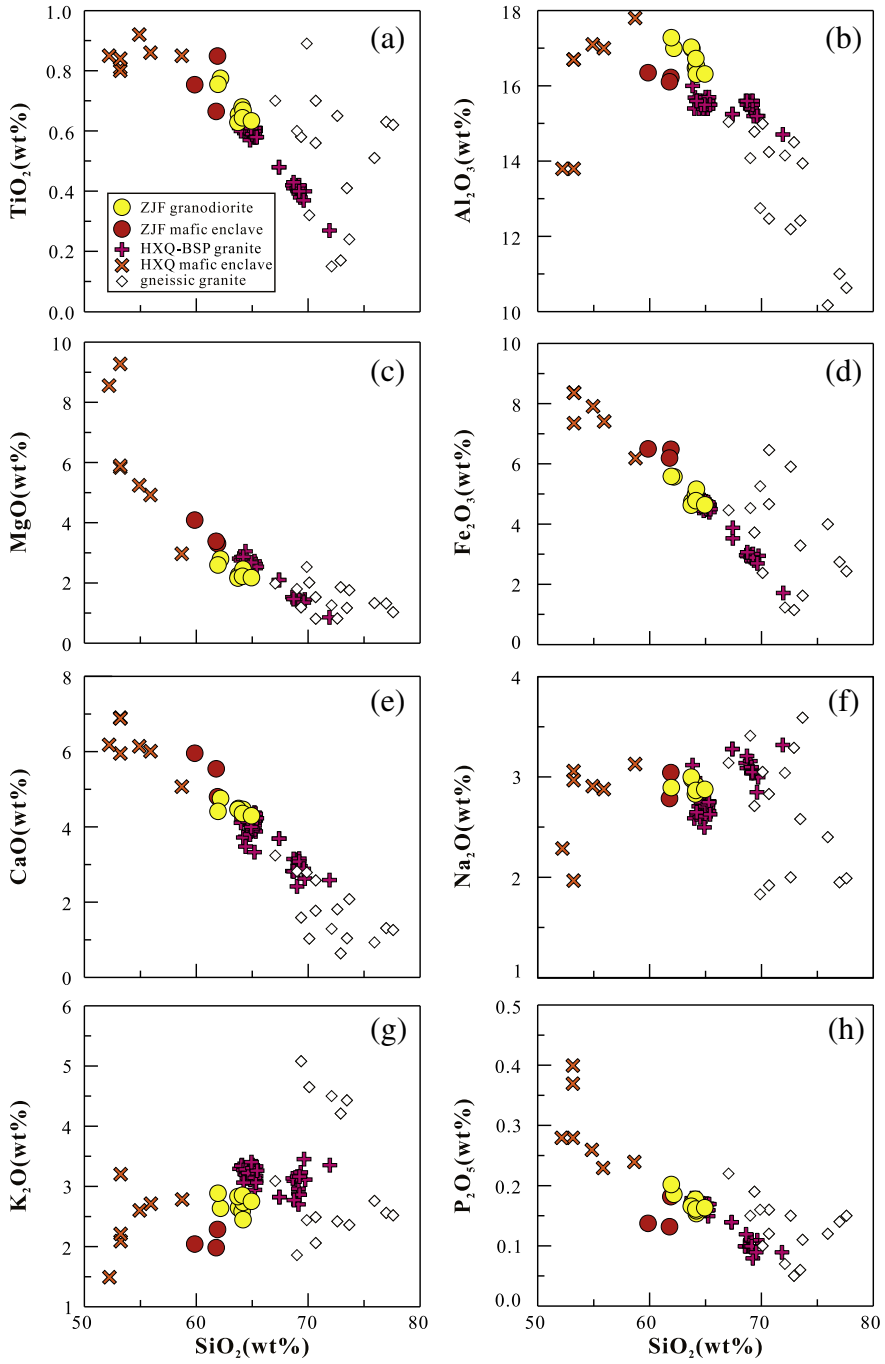

Fig. 6. Harker diagrams for Zhangjiafang (ZJF) granodiorites and MMEs. The data of gneissic granites are from Wang et al. (2011), and those of Banshanpu (BSP) and Hongxiaqiao (HXQ) plutons are from Guan et al. (2014). Gneissic granites include the samples from the Wugongshan, North Wuyi and South Wuyi areas in the Cathaysia Block.

60 wt.%) due to breakdown of plagioclase with amphibole residue in the source (Beard and Lofgren, 1991; Wolf and Wyllie, 1994). Thus, weakly peraluminous feature of the Zhangjiafang granodiorite suggests an overall water-unsaturated partial melting of the source. Low Sr and negative Eu anomalies are consistent with insignificant contribution of plagioclase (Fig. 8a, b), which can also attest to a dehydration melting process.

During dehydration melting of an intermediate-mafic rock (e.g., amphibolite; Beard and Lofgren, 1991), the hydrous phase such as amphibole would break down following different reactions under varying P–T conditions (Wolf and Wyllie, 1994; Wyllie and Wolf, 1993) and supply water for initial melting (Beard and Lofgren, 1991; Douce and Beard, 1995; Wolf and Wyllie, 1994). Garnet together with plagioclase and orthopyroxene would be major residual phase at a high pressure (>8–11 kbar; the pressure varies with the temperature and source composition; Beard and Lofgren, 1991; Wolf and Wyllie, 1994; Wyllie and Wolf, 1993). Nevertheless, the possibility of a high pressure (>8–11 kbar) magma source can be excluded for relatively flat HREE pattern ($[Dy/Yb]_N = 1.22–1.52$; Supplemental Table 3) and high HREE concentration in the Zhangjiafang granodiorite (Fig. 8a). For a mafic source such as amphibolite, amphibole would be a residual phase in the source if thermal gradient is low (Rapp and Watson, 1995; Wolf and Wyllie, 1994), which will induce concave-upward REE patterns between the middle and heavy REEs in the melts (e.g., Huang et al., 2009). The Zhangjiafang granodiorite show a progressive decrease from middle to heavy REEs with increasing atomic number (Fig. 8a),

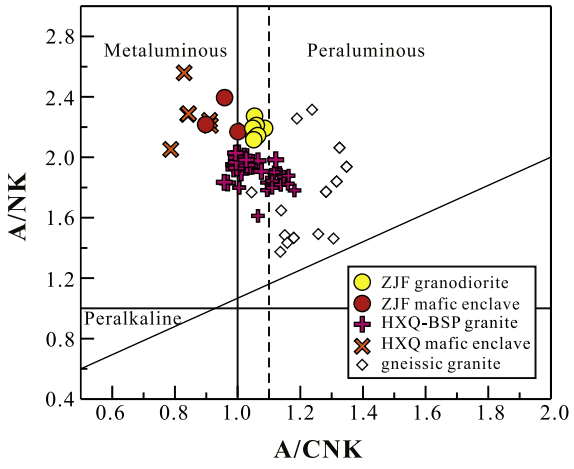

Fig. 7. A/NK vs. A/CNK plots showing metaluminous to weak peraluminous nature of Zhangjiafang (ZJF) granodiorites and MMEs. The data of gneissic granites are from Wang et al. (2011), and those of Banshanpu (BSP) and Hongxiaqiao (HXQ) plutons are from Guan et al. (2014). Gneissic granites include the samples from the Wugongshan, North Wuyi and South Wuyi areas in the Cathaysia Block.

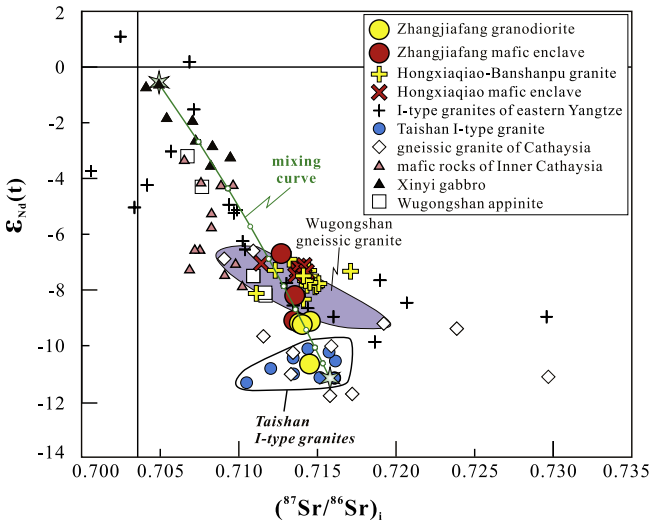

Fig. 9. Initial $\varepsilon_{Nd}(t)$ vs. $(^{87}Sr/^{86}Sr)_i$ for Zhangjiafang granodiorites and MMEs. The data sources: appinites from the Wugongshan area (Zhong et al., 2014), gneissic granites from the Wugongshan, North Wuyi and South Wuyi areas (Wang et al., 2011), I-type granites and coexisting mafic enclave from the Banshanpu and Hongxiaqiao plutons (Guan et al., 2014), other I-type granites of the eastern Yangtze Block (Zhang et al., 2012) and the Taishan pluton (Huang et al., 2013), Xinyi gabbros, and mafic rocks in the inner Cathaysia Block (Wang et al., 2013b; Yao et al., 2012; Zhang et al., 2015). The curve show mixing between mantle derived melts (represented by Xinyi gabbros: Sr = 60 ppm, Nd = 15 ppm, $(^{87}Sr/^{86}Sr)_i = 0.7049$, $\varepsilon_{Nd}(t) = -0.6$) and crustal magma (represented by average value of Taishan I-type granite at Shamaoshi: Sr = 163 ppm, Nd = 33.3 ppm, $(^{87}Sr/^{86}Sr)_i = 0.7158$, $\varepsilon_{Nd}(t) = -11.2$).

thus suggesting the breakdown of amphibole in the source. For a water-unsaturated source in the middle to lower crust (<8 kbar), an extremely high temperature (thermal gradient > 35 °C/km) would be required for the breakdown of amphibole (Huang et al., 2013). However, the Zhangjiafang granodiorite samples have low Zr contents, corresponding to low zircon saturation temperatures (722–780 °C; Supplemental Table 3). Therefore, the Zhangjiafang granodiorite would not be a typical dehydration melting product of the crustal source. The water and heat from mantle-derived melts might have triggered partial melting in the crustal source, which is consistent with variable $\varepsilon_{Nd}(t)$ values of the granodiorite samples (Fig. 9) and abundant MMEs in the pluton (Fig. 3).

5.2. The block boundary between the eastern Yangtze and Cathaysia blocks

The eastern Yangtze and Cathaysia blocks amalgamated during the Early Neoproterozoic (e.g., Li et al., 2006, 2008 2009) and have distinct basements (e.g. Zhang et al., 2012; Zhao and Cawood, 2012). Guan et al. (2014) proposed that the Banshanpu and Hongxiaqiao plutons were derived from partial melting of lower crust of the eastern Yangtze Block in the garnet stability field. In general, the lower crust has low Sr, Ba, Th and U contents because previous partial melting may have extracted such incompatible elements (Rudnick and Fountain, 1995). However, the Banshanpu and Hongxiaqiao plutons show particular high Sr, Ba, Th and U (Fig. 10). In addition, the Daning I-type granite nearby west of Chenzhou–Linwu fault (Fig. 1b) is also characterized by relatively high Ba, Th and U (Fig. 10). The eastern Yangtze Block had been highly modified by extensive juvenile materials during the Neoproterozoic time (e.g., Li et al., 2008 2009; Wang et al., 2004; Yao et al., 2014). The juvenile materials are probably related to the activity of mantle plume associated with breakup of the Rodinia supercontinent (e.g., Li et al., 2009) or breakoff of subducted slab during the post-collision of the Jiangnan orogeny (e.g., Wang et al., 2004). Such a process would be responsible for particular enrichment of Sr, Ba, Th and U in the Banshangpu and Hongxiaqiao plutons (Fig. 10) and overall higher $\varepsilon_{Nd}(t)$ and $\varepsilon_{Hf}(t)$ values of the I-type granites in the eastern Yangtze Block than those in the western Cathaysia Block (Figs. 5, 9).

The Zhangjiafang samples show low Sr, Ba, Th and U contents (Fig. 10), which contradicts with an origin of partial melting of recently modified lower crust similar to the Banshangpu and Hongxiaqiao plutons which is enriched in such incompatible elements. Additionally,

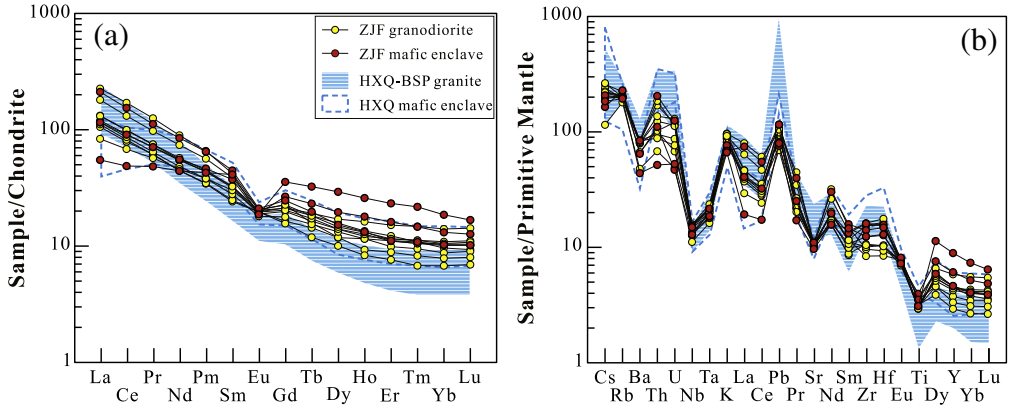

Fig. 8. Chondrite-normalized REE patterns and primitive mantle-normalized trace elements variation diagrams for Zhangjiafang (ZJF) granodiorites and MMEs. Chondrite and PM normalization factors from Taylor and McLennan (1985) and Sun and McDonough (1989), respectively. The data of appinites from Zhong et al. (2014), and those of Banshanpu (BSP) and Hongxiaqiao (HXQ) plutons are from Guan et al. (2014).

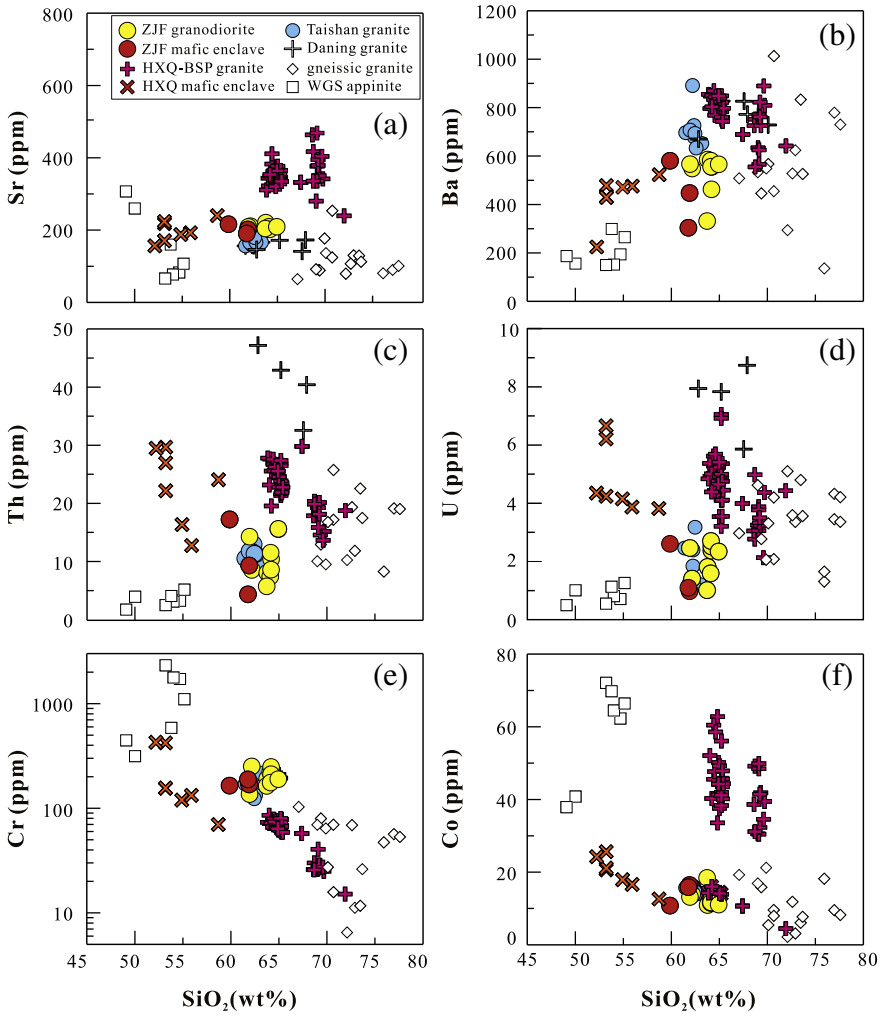

Fig. 10. The diagrams of SiO_2 versus trace elements of Sr, Ba, Th, U, Cr and Co for Zhangjiafang (ZJF) granodiorites and MMEs. The data sources: appinites from the Wugongshan (WGS) area (Zhong et al., 2014), gneissic granites from the Wugongshan (WGS), North Wuyi and South Wuyi areas in the Cathaysia Block (Wang et al., 2011), Daning granite in northeastern Guangxi (Cheng et al., 2009), I-type granites and coexisting mafic enclave from the Banshanpu (BSP) and Hongxiaqiao (HXQ) plutons (Guan et al., 2014).

the Zhangjiafang granodiorite and MME samples have more negative $\varepsilon_{Nd}(t)$ and $\varepsilon_{Hf}(t)$ values than the Banshanpu and Hongxiaqiao plutons in the eastern Yangtze Block, but are similar to the Taishan I-type granitoid rocks in the Cathaysia Block (Figs. 5, 9). The latter was typically derived from partial melting of ancient middle to lower crust of the Cathaysia Block without significant input of juvenile materials (Huang et al., 2013). Although Neoproterozoic event might have significantly affected the eastern part of the Cathysia Block, as revealed by the Neoproterozoic bimodal volcanic rocks along the Zhenghe–Dapu Fault (Shu et al., 2011; Wang et al., 2011), lack of Neoproterozoic rocks in the studied area also suggests an overall undisturbed basement in the western part. Therefore, the Zhangjiafang pluton is mostly produced by partial melting of the basement of the Cathaysia Block. According to contrastive geochemical characteristics of simultaneous I-type granites near the Pingxiang City, we speculated that the block boundary between the Cathaysia and eastern Yangtze blocks would pass through Pingxiang area between the Zhangjiafang pluton and the Banshanpu and Hongxiaqiao plutons (Fig. 1b).

5.3. Origin of the MMEs: insufficient digestion of mantle-derived melts during mixing process

The MMEs would be restite of the source during partial melting (e.g., Chappell and White, 1991; Chappell et al., 1987), "cognate" mafic accumulation in the felsic host (e.g., Dahlquist, 2002; Wall et al., 1987), or mantle-derived melts that injected into and/or mixed insufficiently with felsic magmas (e.g., Barbarin and Didier, 1992; Clemens and Stevens, 2012; Silva et al., 2000). If the MMEs are refractory or residual portions of the source, they should be older than the host rocks and have complementary compositions to the host (e.g., Chappell and White, 1991; Chappell et al., 1987). The Zhangjiafang MMEs show identical crystallization age (Fig. 4d) and similar REE pattern and trace element spiderdiagram to the host granodiorite (Fig. 8), which is inconsistent with the restite model. The model of "cognate" mafic accumulation would not be preferred because the MME samples have distinguishable higher zircon $\varepsilon_{Hf}(t)$ and whole rock $\varepsilon_{Nd}(t)$ but lower whole rock $(^{87}Sr/^{86}Sr)_i$ than the granodiorite samples (Figs. 5, 9).

The Zhangjiafang MMEs and host granodiorites show significant linear trends on the Harker diagrams (Fig. 6) and the diagrams of Nd isotopes versus MgO/Fe_2O_3 and K_2O/Na_2O (Fig. 11), which would indicate a mixing process between mantle-derived and crust-derived melts. The Taishan I-type granites in southern Guangdong (~436 Ma; Fig. 1b) produced by partial melting of ancient middle to lower crust without significant input of juvenile melts (Huang et al., 2013) would be regarded as "pure" melt from the basement of the Cathaysia Block. One Zhangjiafang granodiorite sample has similar $\varepsilon_{Nd}(t)$ value to the Taishan I-type granites (Huang et al., 2013), suggesting similar ancient basement in the north and south parts of the Cathaysia Block. The other granodiorite samples and all MME samples from the Zhangjiafang pluton show less negative $\varepsilon_{Nd}(t)$ values and higher MgO/Fe_2O_3 ratios

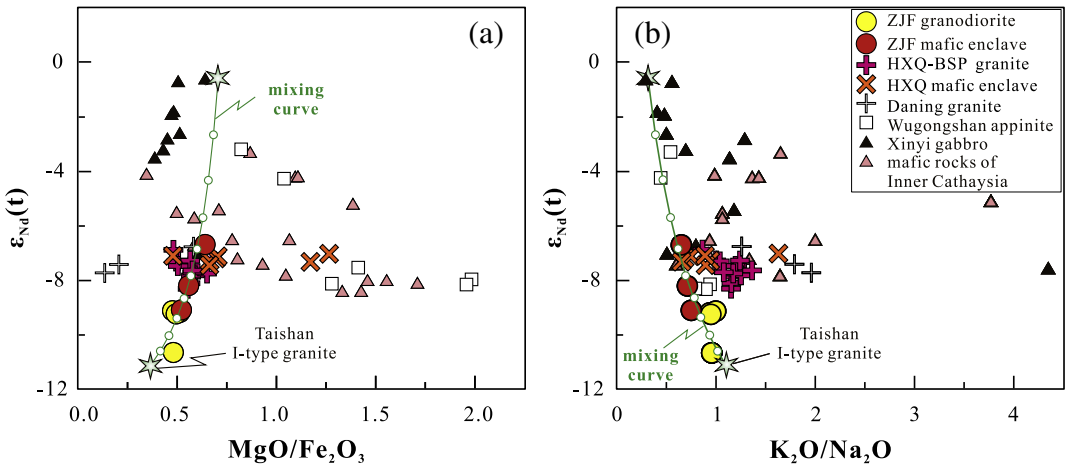

Fig. 11. Initial $\varepsilon_{Nd}(t)$ versus MgO/Fe_2O_3 and K_2O/Na_2O for Zhangjiafang (ZJF) granodiorites and MMEs. Data source: appinites from the Wugongshan (WGS) area (Zhong et al., 2014), I-type granites and coexisting mafic enclave from the Banshanpu (BSP) and Hongxiaqiao (HXQ) plutons (Guan et al., 2014), Daning granite in northeastern Guangxi (Cheng et al., 2009), Xinyi gabbros and other mafic rocks in the inner Cathaysia Block (Wang et al., 2013b; Yao et al., 2012; Zhang et al., 2015). The curves show mixing trend between mantle-derived melts (represented by Xinyi gabbros: Nd = 15 ppm, $\varepsilon_{Nd}(t) = -0.6$, MgO = 7.0 wt.%, Fe_2O_3 = 10.0 wt.%, K_2O = 0.8 wt.%, Na_2O = 2.4 wt.%) and crustal magma (represented by average value of Taishan I-type granite at Shamaoshi: Nd = 33.3 ppm, $\varepsilon_{Nd}(t) = -11.2$, MgO = 2.23 wt.%, Fe_2O_3 = 6.86 wt.%, K_2O = 2.49 wt.%, Na_2O = 2.29 wt.%).

but slightly lower K_2O/Na_2O ratios than the Taishan I-type granites (Fig. 11), reflecting the input of mantle-derived melt. The reported early Paleozoic mafic rocks at present include the nearby appinites in Wugongshan area on the east of Piangxiang (Zhong et al., 2014) and gabbros and basalts in Guangdong and Fujian provinces (Wang et al., 2013b; Yao et al., 2012; Zhang et al., 2015) (Fig. 1b). They all have negative $\varepsilon_{Nd}(t)$ values (Fig. 9) and show pronounced negative Nb–Ta–Ti anomalies (Fig. 8), indicating that they were derived from partial melting of predominant metasomatism mantle source. The Wugongshan appinites, originating from an ancient metasomatised mantle but undergoing crustal assimilation and fractional crystallization (AFC) process (Zhong et al., 2014), have relatively lower $\varepsilon_{Nd}(t)$ values than the gabbros and basalts in Guangdong and Fujian provinces (Fig. 11). The mafic rocks in the inner Cathaysia Block, including the Dakang gabbros, Xinchuan gabbros and Chayuanshan basalts (Fig, 1b), are characterized by variable but overall high MgO/Fe_2O_3 and K_2O/Na_2O ratios and negative $\varepsilon_{Nd}(t)$ values (Fig. 11). The Xinyi gabbros adjacent to the block boundary in the Yunkai domain (Fig. 1b) show overall lower MgO/Fe_2O_3 and K_2O/Na_2O ratios and less negative $\varepsilon_{Nd}(t)$ values than the mafic rocks in the inner Cathaysia Block (Fig. 11), indicating a "younger" lithosphere mantle source beneath the marginal region compared with the inner Cathaysia Block. The Zhangjiafang granodiorites and MMEs have relatively low MgO/Fe_2O_3 and K_2O/Na_2O ratios and plot on the mixing trend between the Xinyi gabbros and Taishan I-type granites (Figs. 9, 11), indicating that they would be insufficient mixture of similar ultimate sources. Evidently, the Zhangjiafang MMEs contain irregular granitoid veinlets (Fig. 3b) and variable amounts of large-grained xenocrysts or clots of quartz and feldspar. Therefore, the Zhangjiafang MMEs were likely mantle-derived melts injected into felsic magmas without complete digestion.

5.4. Implication for the collapse of the Wuyi–Yunkai orogen

The Wuyi–Yunkai orogen has been regarded as a consequence of continental or arc collisions with closure of a proposed Huanan Ocean in the SCB interior (e.g., Guo et al., 1989; Hsü, 1994; Hsü et al., 1990). But most recent work interpreted the Wuyi–Yunkai orogen as an intracontinental event (Charvet, 2013; Charvet et al., 2010; Faure et al., 2009; Guan et al., 2014; Huang et al., 2013; Li et al., 2010; Wang et al., 2007, 2011, 2013b; Yao et al., 2012). Lack of juvenile component in the early Paleozoic crust of the SCB (e.g., Huang et al., 2013; Wang et al., 2011, 2013a) suggests an overall undisturbed crust prior to orogeny but distinctly contradicts the model of an early Paleozoic Huanan Ocean between the Cathaysia and Yangtze blocks (e.g., Guo et al., 1989; Hsü, 1994; Hsü et al., 1990). A far-field-type intracontinental orogenic collapse would have occurred in the early Paleozoic (Li et al., 2010), which had a strong heat influence on crustal mobilization beneath the inner Cathaysia Block (Huang et al., 2013). The Zhangjiafang pluton adjacent to the block boundary between the eastern Yangtze and Cathaysia blocks also show insignificant juvenile materials in its crustal source prior to the orogeny, obviously preferring an intracontinental orogeny model.

Intracontinental orogeny is closely related to the reactivation of ancient thrusting structures or pre-existing lithospheric weak zones (Hand and Sandiford, 1999; Sandiford and Hand, 1998), such as the Cenozoic Tianshan Belt in Central Asia (Yin et al., 1998), the late Neoproterozoic Peterman orogen and the Paleozoic Alice Springs orogen in Central Australia (Hand and Sandiford, 1999; Sandiford and Hand, 1998). The Wuyi–Yunkai orogen had experienced a clockwise P–T path with rapid pressure drop from >8 kbar during 460–440 Ma to ~4 kbar after 440 Ma (Li et al., 2010), suggesting a tectonic transition from compression to extension in accordance with a far-field-type intracontinental orogenic collapse in the early Paleozoic (Li et al., 2010). Asthenosphere upwelling during post-orogenic collapse could input significant heat and mafic melts into the crust and might result in large-scale granitic magmatism (Gorczyk and Vogt, 2015; Huang et al., 2013; Smithies et al., 2011). The early Paleozoic I-type granites and mafic rocks in the SCB all occurred after 440 Ma, which would be a witness for the remobilization of the crustal basement associated with partial melting of lithospheric mantle during post-orogenic collapse (Fig. 1b). The mixing process recorded in the Zhangjiafang pluton reflects the direct modification of mantle-derived melt on the ancient basement in the northern margin of the Cathaysia Block due to the collapse of the Wuyi–Yunkai orogen. It is noteworthy that the early Paleozoic mafic rocks (Wang et al., 2013b; Zhong et al., 2014) and I-type granites with coeval MMEs (Guan et al., 2014; this study) were frequently present along the Jiangshan–Shaoxing–Pingxiang–Chenzhou–Linwu Fault zone which would be in juxtaposition with the block boundary (Fig. 1b). This strongly suggests that the pre-existing block boundary or fault might have played an important role on the collapse of the Wuyi–Yunkai orogen. Actually, most of the I-type granites near the block boundary show the mixing process between mafic and felsic melts (Guan et al., 2014; Xia et al., 2014; Zhang et al., 2012; this study). Therefore, the pre-existing block boundary may be a proper location for the juxtaposition of asthenospheric upwelling and basaltic underplating (Fig. 12) during the collapse of an intracontinental orogen.

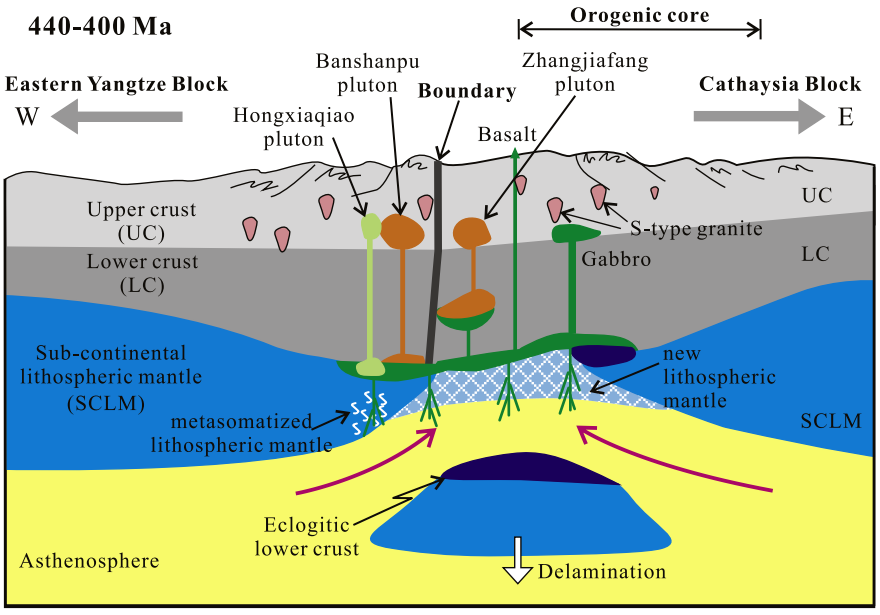

Fig. 12. Cartoon showing the asthenospheric upwelling, basaltic underplating and associated magmatism along the pre-existing boundary between eastern Yangtze and Cathaysia blocks during the collapse of the Wuyi–Yunkai orogen.

6. Conclusion

(1) The Zhangjiafang granodiorites in the northern margin of the Cathaysia Block are typical early Paleozoic I-type granitoid rocks derived from partial melting of the basement of the Cathaysia Block.
(2) The MMEs in the Zhangjiafang pluton were ultimately mantle-derived melts but had experienced incomplete mixing process.
(3) The basement of Cathaysia Block is more ancient than that of the eastern Yangtze Block. The block boundary between the Cathaysia and eastern Yangtze blocks passes through the nearby west area (i.e., Pingxiang City) of the Zhangjiafang pluton.
(4) Pre-existing block boundary is a proper location for juxtaposition of asthenosphere upwelling and basaltic underplating during the collapse of an intracontinental orogen.

Supplementary data to this article can be found online at http://dx.doi.org/10.1016/j.lithos.2016.02.002.

Acknowledgment

We thank C.Y. Li, X.R. Liang, Y. Liu and X.L. Tu for their analytical assistance. We acknowledge the constructive comments of Prof. L.S. Shu and two anonymous reviewers, which helped considerably in improving the manuscript. This research was financially supported by the National Basic Research Program of China (973 Program: 2012CB416703) and the National Science Foundation of China (NSFC Projects 41130314, 91214202, 41373032). This is contribution No. IS-2189 to GIG-CAS.

References

Barbarin, B., Didier, J., 1992. Genesis and evolution of mafic microgranular enclaves through various types of interaction between coexisting felsic and mafic magmas. Transactions of the Royal Society of Edinburgh: Earth Sciences 83, 145–153.
Beard, J.S., Lofgren, G.E., 1991. Dehydration melting and water-saturated melting of basaltic and andesitic greenstones and amphibolites at 1, 3, and 6.9 kbar. Journal of Petrology 32, 365–401.
Black, L.P., Kamo, S.L., Allen, C.M., Aleinikoff, J.N., Davis, D.W., Korsch, R.J., Foudoulis, C., 2003. TEMORA 1: a new zircon standard for Phanerozoic U–Pb geochronology. Chemical Geology 200, 155–170.
Blichert-Toft, J., Albarede, F., 1997. The Lu–Hf geochemistry of the chondrites and the evolution of the mantle–crust system. Earth and Planetary Science Letters 148, 243–258.
Chappell, B.W., White, A.J.R., 1991. Restite enclaves and the restite model. In: Didier, J., Barbarin, B. (Eds.), Enclaves and Granite Petrology, Developments in Petrology. Elsevier, Amsterdam, pp. 375–381.
Chappell, B.W., White, A.J.R., Wyborn, D., 1987. The importance of residual source material (restite) in granite petrogenesis. Journal of Petrology 28, 1111–1138.
Charvet, J., 2013. The Neoproterozoic–Early Paleozoic tectonic evolution of the South China Block: an overview. Journal of Asian Earth Sciences 74, 198–209.
Charvet, J., Shu, L.S., Faure, M., Choulet, F., Wang, B., Lu, H.F., Breton, N.L., 2010. Structural development of the Lower Paleozoic belt of South China: genesis of an intracontinental orogen. Journal of Asian Earth Sciences 39, 309–330.
Chen, J.F., Foland, K.A., Xing, F.M., Xu, X.A., Zhou, T.X., 1991. Magmatism along the southeast margin of the Yangtze block: Precambrian collision of the Yangtze and Cathysia blocks of China. Geology 19, 815–818.
Chen, C.H., Lee, C.Y., Hsieh, P.S., Zeng, W., Zhou, H.W., 2008. Approaching the age problem for some metamorphosed Precambrian basement rocks and Phanerozoic granitic bodies in the Wuyishan area: the application of EMP monazite age dating. Geological Journal of China Universities 14 (1), 1–15.
Chen, X., Zhang, Y.D., Fan, J.X., Tang, L., Sun, H.Q., 2012. Onset of the Kwangsian Orogeny as evidenced by biofacies and lithofacies. Science China Earth Sciences 55, 1592–1600.
Cheng, S.B., Fu, J.M., Xu, D.M., Chen, X.Q., Ma, L.Y., Wang, X.D., Pang, Y.C., 2009. Zircon SHRIMP U–Pb dating and geochemical characteristics of Daning batholith in northeast Guangxi. Geology in China 36 (6), 1278–1288 (in Chinese with English abstract).
Clemens, J.D., Stevens, G., 2012. What controls chemical variation in granitic magmas? Lithos 134, 317–329.
Dahlquist, J.A., 2002. Mafic microgranular enclaves: early segregation from metaluminous magma (Sierra de Chepes), Pampean Ranges, NW Argentina. Journal of South America Earth Science 15, 643–655.
Douce, A.E.P., Beard, J.S., 1995. Dehydration-melting of biotite gneiss and quartz amphibolite from 3 to 15 kbar. Journal of Petrology 36, 707–738.
Faure, M., Shu, L.S., Wang, B., Charvet, J., Choulet, F., Monié, P., 2009. Intracontinental subduction: a possible mechanism for the Early Paleozoic Orogen of SE China. Terra Nova 21, 360–368.
Gan, X.C., Li, H.M., Sun, D.Z., Zhuang, J.M., 1993. Geochronological study on the Precambrian metamorphic basement in Northern Fujian. Geology of Fujian 17, 17–32 (in Chinese with English abstract).
Gao, S., Yang, J., Zhou, L., Li, M., Hu, Z.C., Guo, J.L., Yuan, H.L., Gong, H.J., Xiao, G.Q., Wei, J.Q., 2011. Age and growth of the Archean Kongling terrain, South China, with emphasis on 3.3 Ga granitoid gneisses. American Journal of Science 311, 153–182.
Gerdes, A., Zeh, A., 2006. Combined U–Pb and Hf isotope LA-(MC-)ICP-MS analyses of detrital zircons: Comparison with SHRIMP and new constraints for the provenance and age of an Armorican metasediment in Central Germany. Earth and Planetary Science Letters 249, 47–61.
Gorczyk, W., Vogt, K., 2015. Tectonics and melting in intra-continental settings. Gondwana Research 27, 196–208.
Guan, Y.L., Yuan, C., Sun, M., Wilde, S., Long, X.P., Huang, X.L., Wang, Q., 2014. I-type granitoids in the eastern Yangtze Block: implications for the Early Paleozoic intracontinental orogeny in South China. Lithos 206, 34–51.
Guo, L.Z., Shi, Y.S., Lu, H.F., Ma, S.R., Dong, H.G., Yang, S.F., 1989. The pre-Devonian tectonic patterns and evolution of South China. Journal of Southeast Asian Earth Sciences 3, 87–93.
Hand, M., Sandiford, M., 1999. Intraplate deformation in central Australia, the link between subsidence and fault reactivation. Tectonophysics 305, 121–140.

Hsü, K.J., 1994. Tectonic facies in an archipelago model of intra-plate orogenesis. GSA Today 4 (12), 289–293.
Hsü, K.J., Li, J.L., Chen, H.H., Wang, Q.C., Sun, S., Sengör, A.M.X., 1990. Tectonics of South China: key to tectonics of South China: key to understanding west Pacific geology. Tectonophysics 193, 9–39.
Huang, X.L., Xu, Y.G., Lan, J.B., Yang, Q.J., Luo, Z.Y., 2009. Neoproterozoic adakitic rocks from Mopanshan in the western Yangtze Craton: partial melts of a thickened lower crust. Lithos 112, 367–381.
Huang, X.L., Yu, Y., Li, J., Tong, L.X., Chen, L.L., 2013. Geochronology and petrogenesis of the early Paleozoic I-type granite in the Taishan area, South China: middle-lower crustal melting during orogenic collapse. Lithos 177, 268–284.
Iizuka, T., Hirata, T., 2005. Improvements of precision and accuracy in in-situ Hf isotope microanalysis of zircon using the laser ablation-MC-ICPMS technique. Chemical Geology 220, 121–137.
Lebreton, N., Thompson, A.B., 1988. Fluid-absent (dehydration) melting of biotite in metapelites in the early stages of crustal anatexis. Contributions to Mineralogy and Petrology 99, 226–237.
Li, X.H., Li, Z.X., Wingate, M.T.D., Chung, S.L., Liu, Y., Lin, G.C., Li, W.X., 2006. Geochemistry of the 755 Ma Mundine Well dyke swarm, northwestern Australia: part of a Neoproterozoic mantle superplume beneath Rodinia? Precambrian Research 146, 1–15.
Li, W.X., Li, X.H., Li, Z.X., Lou, F.S., 2008. Obduction-type granites within the NE Jiangxi Ophiolite: implications for the final amalgamation between the Yangtze and Cathaysia Blocks. Gondwana Research 13, 288–301.
Li, X.H., Li, W.X., Li, Z.X., Lo, C.H., Wang, J., Ye, M.F., Yang, Y.H., 2009. Amalgamation between the Yangtze and Cathaysia Blocks in South China: constraints from SHRIMP U–Pb zircon ages, geochemistry and Nd–Hf isotopes of the Shuangxiwu volcanic rocks. Precambrian Research 174, 117–128.
Li, Z.X., Li, X.H., Wartho, J.A., Clark, C., Li, W.X., Zhang, C.L., Bao, C., 2010. Magmatic and metamorphic events during the Early Paleozoic Wuyi–Yunkai Orogeny, southeastern South China: new age constraints and pressure–temperature conditions. Geological Society of America Bulletin 122, 772–793.
Liang, X.R., Wei, G.J., Li, X.H., Liu, Y., 2003. Precise measurement of $^{143}Nd/^{144}Nd$ and Sm/Nd ratios using multiple-collectors inductively couple plasma-mass spectrometer (MC-ICP-MS). Geochimica 32, 91–96 (in Chinese with English abstract).
Liu, Y.S., Hu, Z.C., Gao, S., Gunther, D., Xu, J., Gao, C.G., Chen, H.H., 2008. In situ analysis of major and trace elements of anhydrous minerals by LA-ICP-MS without applying an internal standard. Chemical Geology 257, 34–43.
Liu, Q., Yu, J.H., O'Reilly, S.Y., Zhou, M.F., Griffin, W.L., Wang, L.J., Cui, X., 2014. Origin and geological significance of Paleoproterozoic granites in the northeastern Cathaysia Block, South China. Precambrian Research 248, 72–95.
Lou, F.S., Shen, W.Z., Wang, D.Z., Shu, L.S., Wu, F.J., Zhang, F.R., Yu, J.H., 2005. Zircon U–Pb isotopic chronology of the Wugongshan dome compound granite in Jiangxi Province. Acta Geologica Sinica 5, 636–644 (in Chinese with English abstract).
Ludwig, K.R., 2003. Isoplot: a geochronological toolkit for Microsoft Excel. Berkeley Geochronology Center Special Publication 4, 1–67.
McArthur, J.M., 1994. Recent trends in strontium isotope stratigraphy. Terra Nova 6, 331–358.
Pearce, N.J.G., Perkins, W.T., Westgate, J.A., Grrton, M.P., Jackson, S.E., Neal, C.R., Chenery, S.P., 1997. A compilation of new and published major and trace element data for NIST SRM 610 and NIST SRM 612 glass reference materials. Geostandards Newsletter 21, 115–144.
Peng, S.B., Jin, Z.M., Liu, Y.H., Fu, J.M., He, L.Q., Cai, M.H., Wang, Y.B., 2006. Petrochemistry, chronology and tectonic setting of strong peraluminous anatectic granitoids in Yunkai Orogenic Belt, Western Guangdong Province, China. Journal of China University of Geosciences 17, 1–12 (in Chinese with English abstract).
Qiu, Y.M., Gao, S., McNaughton, N.J., Groves, D.J., Ling, W.L., 2000. First evidence of ≥3.2 Ga continental crust in the Yangtze craton of South China and its implications for Archean crustal evolution and Phanerozoic tectonics. Geology 28, 11–14.
Rao, J.R., Xiao, H.Y., Liu, Y.R., Bai, D.Y., Deng, Y.Y., 2012. Location of the Yangtze–Cathaysia plate convergence zone in Hunan. Chinese Journal of Geophysics 55, 484–502 (Chinese Edition).
Rapp, R.P., Watson, E.B., 1995. Dehydration melting of metabasalt at 8–32 kbar: implications for continental growth and crust–mantle recycling. Journal of Petrology 36, 891–931.
Rudnick, R.L., Fountain, D.M., 1995. Nature and composition of the continental crust: a lower crustal perspective. Review of Geophysics 33, 267–309.
Sandiford, M., Hand, M., 1998. Controls on the locus of intraplate deformation in central Australia. Earth and Planetary Science Letters 162, 97–110.
Scherer, E., Munker, C., Mezger, K., 2001. Calibration of the Lutetium–Hafnium clock. Science 293, 683–687.
Shen, W.Z., Zhang, F.R., Shu, L.S., Wang, L.J., Xiang, L., 2008. Formation age, geochemical characteristics of the Ninggang granite body in Jiangxi Province and its tectonic significance. Acta Petrologica Sinica 24, 2244–2254 (in Chinese with English abstract).
Shu, L.S., Faure, M., Yu, J.H., Jahn, B.M., 2011. Geochronological and geochemical features of the Cathaysia block (South China): new evidence for the Neoproterozoic breakup of Rodinia. Precambrian Research 187, 263–276.
Shu, L.S., Jahn, B.M., Charvet, J., Santosh, M., Wang, B., Xu, X.S., Jiang, S.Y., 2014. Early Paleozoic depositional environment and intraplate tectono-magmatism in the Cathaysia Block (South China): evidence from stratigraphic, structural, geochemical and geochronological investigations. American Journal of Science 314, 154–186.
Shu, L.S., Wang, B., Cawood, P.A., Santosh, M., Xu, Z.Q., 2015. Early Paleozoic and early Mesozoic intraplate tectonic and magmatic events in the Cathaysia Block, South China. Tectonics 34. http://dx.doi.org/10.1002/2015TC003835.
Shui, T., 1987. Tectonic framework of the southeastern China continental basement. Scientia Sinica B30, 414–422.
Silva, M.M.V.G., Neiva, A.M.R., Whitehouse, M.J., 2000. Geochemistry of enclaves and host granites from the Nelas area, central Portugal. Lithos 50, 153–170.
Smithies, R.H., Howard, H.M., Evins, P.M., Kirkland, C.L., Kelsey, D.E., Hand, M., Wingate, M.T.D., Collins, A.S., Belousova, E., 2011. High-temperature granite magmatism, crust–mantle interaction and the Mesoproterozoic intracontinental evolution of the Musgrave Province, Central Australia. Journal of Petrology 52, 931–958.
Sun, S.S., McDonough, W.F., 1989. Chemical and isotopic systematics of oceanic basalts: implication for mantle composition and process. In: Sauders, A.D., Norry, M.J. (Eds.), Magmatism in the Ocean Basins. Geological Society Specical Publications 42, pp. 313–345.
Tannaka, T., Togashi, S., Kamioka, H., Amakawa, H., Kagami, H., Hamamoto, T., Yuhara, M., Orihashi, Y., Yoneda, S., Shimizu, H., Kunimaru, T., Takahashi, K., Yanagi, T., Nakano, T., Fujimaki, H., Shinjo, R., Asahara, Y., Tanimizu, M., Dragusanu, C., 2000. JNdi-1: a neodymium isotopic reference in consistency with LaJolla neodymium. Chemical Geology 168, 279–281.
Taylor, S.R., McLennan, S.M., 1985. The Continental Crust: Its Composition and Evolution. Blackwell, Oxford.
Tu, X.L., Zhang, H., Deng, W.F., Ling, M.X., Liang, H.Y., Liu, Y., Sun, W.D., 2011. Application of RESOlution in-situ laser ablation ICP-MS in trace element analyses. Geochemica 40 (1), 83–98 (in Chinese with English abstract).
Vielzeuf, D., Montel, J.M., 1994. Partial melting of metagreywackes, part II. Compositions of minerals and melts. Contributions to Mineralogy and Petrology 117, 375–393.
Wall, V.J., Clemens, J.D., Clarke, D.B., 1987. Models for granitoid evolution and source compositions. Journal of Geology 95, 731–749.
Wan, Y.S., Liu, D.Y., Xu, M.H., Zhuang, J.M., Song, B., Shi, Y.R., Du, L.L., 2007. SHRIMP U–Pb zircon geochronology and geochemistry of metavolcanic and metasedimentary rocks in North western Fujian, Cathaysia Block, China: tectonic implications and the need to redefine lithostratigraphic units. Gondwana Research 12, 166–183.
Wan, Y.S., Liu, D.Y., Simon, A.W., Cao, J.J., Chen, B., Dong, C.Y., 2010. Evolution of the Yunkai terrane, South China: evidence from SHRIMP zircon U–Pb dating, geochemistry and Nd isotope. Journal of Asian Earth Sciences 37, 140–153.
Wang, Y.J., Fan, W.M., Guo, F., Peng, T.P., Li, C.W., 2003. Geochemistry of Mesozoic mafic rocks around the Chenzhou–Linwu fault in South China: implication for the lithospheric boundary between the Yangtze and the Cathaysia Blocks. International Geology Review 45, 263–286.
Wang, X.L., Zhou, J.C., Qiu, J.S., Gao, J.F., 2004. Geochemistry of the Meso- to Neoproterozoic basic-acid rocks from Hunan Province, South China: implications for the evolution of the western Jiangnan orogen. Precambrian Research 135, 79–103.
Wang, Y.J., Fan, W.M., Zhao, G.C., Ji, S.C., Peng, T.P., 2007. Zircon U–Pb geochronology of gneissic rocks in the Yunkai massif and its implications on the Caledonian event in the South China Block. Gondwana Research 12, 404–416.
Wang, Y.J., Zhang, A.M., Fan, W.M., Zhao, G.C., Zhang, G.W., Zhang, F.F., Zhang, Y.Z., Li, S.Z., 2011. Kwangsian crustal anatexis within the eastern South China Block: geochemical, zircon U–Pb geochronological and Hf isotopic fingerprints from the gneissoid granites of Wugong and Wuyi–Yunkai domains. Lithos 127, 239–260.
Wang, X.L., Shu, L.S., Xing, G.F., Zhou, J.C., Tang, M., Shu, X.J., Qi, L., Hu, Y.H., 2012. Post-orogenic extension in the eastern part of the Jiangnan orogen: evidence from ca 800–760 Ma volcanic rocks. Precambrian Research 222–223, 404–423.
Wang, Y.J., Fan, W.M., Zhang, G.W., Zhang, Y.H., 2013a. Phanerozoic tectonics of the South China Block: Key observations and controversies. Gondwana Research 23, 1273–1305.
Wang, Y.J., Zhang, A.M., Fan, W.M., Zhang, Y.H., Zhang, Y.Z., 2013b. Origin of paleosubduction-modified mantle for Silurian gabbro in the Cathaysia Block: geochronological and geochemical evidence. Lithos 160–161, 37–54.
Wang, Y.J., Zhang, A.M., Cawood, F.A., Fan, W.M., Xu, J.F., Zhang, G.W., Zhang, Y.Z., 2013c. Geochronological, geochemical and Nd–Hf–Os isotopic fingerprinting of an early Neoproterozoic arc–back-arc system in South China and its accretionary assembly along the margin of Rodinia. Precambrian Research 231, 343–371.
Wei, G.J., Liang, X.R., Li, X.H., Liu, Y., 2002. Precise measurement of Sr isotopic compositions of liquid and solid base using (LA) MC-ICP-MS. Geochimica 31, 295–305 (in Chinese with English abstract).
Whalen, J.B., 1985. Geochemistry of an island-arc plutonic suite: the Uasilau-Yau Yau intrusive complex, New Britain P.N.G. Journal of Petrology 26, 603–632.
Wolf, M.B., Wyllie, P.J., 1994. Dehydration-melting of amphibolite at 10 kbar: the effects of temperature and time. Contributions to Mineralogy and Petrology 115, 369–383.
Woodhead, J., Hergt, J., Shelley, M., Eggins, S., Kemp, R., 2004. Zircon Hf-isotope analysis with an excimer laser, depth profiling, ablation of complex geometries, and concomitant age estimation. Chemical Geology 209, 121–135.
Wu, F.J., Zhang, F.R., 2003. Features and genesis of Caledonian granites in the Wugong in the eastern segment of the northern margin of South China. Geology in China 30, 166–172 (in Chinese with English abstract).
Wu, F.Y., Yang, Y.H., Xie, L.W., Yang, J.H., Xu, P., 2006. Hf isotopic compositions of the standard zircons and baddeleyites used in U–Pb geochronology. Chemical Geology 234, 105–126.
Wyllie, P.J., Wolf, M.B., 1993. Amphibolite dehydration-melting: sorting out the solidus. Geological Society, London, Special Publications 76, 405–416.
Xia, Y., Xu, X.S., Zou, H.B., Liu, L., 2014. Early Paleozoic crust–mantle interaction and lithosphere delamination in South China Block: evidence from geochronology, geochemistry, and Sr–Nd–Hf isotopes of granites. Lithos 184–187, 416–435.
Xie, Z.D., Yang, Y.G., 2000. Isotopic age of zircon in Anxi pluton of Xinfeng, Jiangxi, and its geological implications. Jiangxi Geology 14 (3), 172–175 (in Chinese with English abstract).
Xu, W.J., Xu, X.S., 2015. Early Paleozoic intracontinental felsic magmatism in the South China Block: petrogenesis and geodynamics. Lithos 234–235, 79–92.
Xu, X.S., O'Reilly, S.Y., Griffin, W.L., Deng, P., Pearson, N.J., 2005. Relict Proterozoic basement in the Nanling Mountains (SE China) and its tectonothermal overprinting. Tectonics 24, 1–16.

Xu, X.B., Zhang, Y.Q., Shu, L.S., Jia, D., Wang, R.R., Xu, H.Z., 2009. Zircon LA-ICP-MS U–Pb dating of the Weipu granitic pluton in southwest Fujian and the Changpu migmatite in South Jiangxi: constrains to the timing of Caledonian movement in Wuyi mountains. Geological Review 55, 277–285 (in Chinese with English abstract).

Yao, W.H., Li, Z.X., Li, W.X., Wang, X.C., Li, X.H., Yang, J.H., 2012. Post-kinematic lithospheric delamination of the Wuyi–Yunkai orogen in South China: evidence from ca. 435 Ma high-Mg basalts. Lithos 154, 115–129.

Yao, J.L., Shu, L.S., Santosh, M., 2014. Neoproterozoic arc-trench system and breakup of the South China Craton: constraints from N-MORB type and arc-related mafic rocks, and anorogenic granite in the Jiangnan orogenic belt. Precambrian Research 247, 187–207.

Yin, A., Nie, S., Craig, P., Harrison, T.M., Ryerson, F.J., Xianglin, Q., Geng, Y., 1998. Late Cenozoic tectonic evolution of the southern Chinese Tian Shan. Tectonics 17, 1–27.

Yu, J.H., Wang, L.J., O'Reilly, S.Y., Griffin, W.L., Zhang, M., Li, C.Z., Shu, L.S., 2009. A Paleoproterozoic orogeny recorded in a long-lived cratonic remnant (Wuyishan terrane), eastern Cathaysia Block, China. Precambrian Research 174, 347–363.

Yu, J.H., O'Reilly, S.Y., Wang, L.J., Griffin, W.L., Zhou, M.F., Zhang, M., Shu, L.S., 2010. Components and episodic growth of Precambrian crust in the Cathaysia Block, South China: evidence from U–Pb ages and Hf isotopes of zircons in Neoproterozoic sediments. Precambrian Research 181, 97–114.

Zhang, F.F., Wang, Y.J., Zhang, A.M., Fan, W.M., Zhang, Y.Z., Zi, J.W., 2012. Geochronological and geochemical constraints on the petrogenesis of Middle Paleozoic (Kwangsian) massive granites in the eastern South China Block. Lithos 150, 188–208.

Zhang, Q., Jiang, Y.H., Wang, G.C., Liu, Z., Ni, C.Y., Qing, L., 2015. Origin of Silurian gabbros and I-type granites in central Fujian, SE China: implications for the evolution of the early Paleozoic orogen of South China. Lithos 216–217, 285–297.

Zhao, G.C., Cawood, P.A., 2012. Precambrian geology of China. Precambrian Research 222–223, 13–54.

Zhao, L., Zhou, X.W., Zhai, M.G., Santosh, M., Geng, Y.S., 2014. Zircon U–Th–Pb–Hf isotopes of the basement rocks in northeastern Cathaysia Block, South China: implications for Phanerozoic multiple metamorphic reworking of a Paleoproterozoic terrane. Gondwana Research 28, 246–261.

Zhong, Y.F., Ma, C.Q., Liu, L., Zhao, J.H., Zheng, J.P., Nong, J.N., Zhang, Z.J., 2014. Ordovician appinites in the Wugongshan domain of the Cathaysia Block, South China: Geochronological and geochemical evidence for intrusion into a local extensional zone within an intracontinental regime. Lithos 198, 201–216.